PROCESS MONITORING BASED ON MEASUREMENT SPACE DECOMPOSITION

José L. Godoy[(a)], Jorge R. Vega[(a)(b)] and Jacinto L. Marchetti[(a)]

[(a)] INTEC (CONICET-Universidad Nacional del Litoral), Güemes 3450, 3000, Santa Fe, Argentina
[(b)] Facultad Regional Santa Fe, UTN, Lavaisse 610, 3000, Santa Fe, Argentina

[(a)]jlgodoy@santafe-conicet.gov.ar, jvega@santafe-conicet.gov.ar, jlmarch@santafe-conicet.gov.ar.

ABSTRACT
A useful decomposition of the input and output variable spaces is obtained by using the relationships supporting Partial Least Squares Regression (PLSR). The resulting technique is capable to classify faults or anomalies according to four types: those associated to measurements of input variables, those related to measurements of output variables, those linked to the inner latent structure of the complex processes data and those related to upsets that follow its correlation structure. This classification is suggested by the different subspaces in which the whole measurement space can be decomposed by using PLSR modeling and specific statistics actuating on each subspace. Hence, using an in-control PLSR model, the tool is able to detect anomalies and to diagnose its kind. The approach can be used for monitoring closed loop systems and to detect abnormal controller functioning. Several features of the proposed classification technique are analyzed through static and dynamic simulation examples.

Keywords: PLSR, space decomposition, multivariate process monitoring, fault detection indexes.

1. INTRODUCTION

The need for associating input and output data sets obtained by online data login of several variables originated in complex processes constitutes a problem that requires increasing attention. Monitoring strategies are used in industry to detect and diagnose abnormal processes behavior. Fault detection indices are lately being proposed to indicate abnormalities in process operations: a fault signal appears basically when one single or combined index goes beyond its control limit. After a fault is detected, the need of having a diagnostic about its cause becomes almost mandatory. Typically, this diagnostic is performed by analyzing the contributions made by each measured variable to the index has given the alarm.

Lately, PLSR has become a powerful approach to find multivariable linear structures in the data, mainly because significant co-linearity, which is frequently implicit in there, can be adequately overcome.

Nowadays, the chemical process industries appeal to multivariable control technologies for controlling complex multi-input multi-output (MIMO) processes systems. However, in general, it is clear that not only multivariable control systems but also traditional multi-loop control systems must be monitored for improving quality and performance standards and for stabilizing production throughputs. Hence, monitoring medium or large processes to detect abnormalities or undesirable low performances has become an important research field.

As mentioned before, the multivariate nature of most processes frequently shows highly correlated variables. However, they usually move in an effective subspace of lower dimension, this is because latent variable (LV) methods can transform noisy and correlated data into a smaller informative set free of ill-conditionings. Since PLSR lays on a reduced set of input-output LV's, it allows fitting a MIMO linear model using an identification data set that might have been originally ill-conditioned.

Lately, some applications based on PCA/PLS are being done through data acquisition systems collecting measurements directly from the plant. An important contribution in this area was provided by AlGazzawi and Lennox (2009), who investigated the ability of multivariate statistical process control (MSPC) techniques to monitor industrial model predictive control (MPC) systems. This has also encouraged the development of a data-driven LV-MPC method, where PLSR is used for fitting a multi-step ahead prediction model and the MPC is then implemented in the space of the LV's (Laurí et al., 2010). This type of works confirms the actual efforts to improving the way of managing multivariable data sets.

This work attempts a contribution in this area by providing an online data processing technique capable of orientating process engineers towards the main causes of alarming faults signals and undesirables performances. Hence, the presentation is as follow: in Section 2 we recall the main relationships arising when developing a PLSR model; in particular the Sub-section 2.1 formalizes the PLSR implicit decomposition and describes several geometric properties useful for better understanding of the contribution. In Section 3 the main statistical tools are introduced and their roll in the measurement decomposition is described. Sub-section 3.2 and the numerical application example in Sub-section 4.1 have a core importance in understanding the proposed technique. Sub-section 4.2 presents a more realistic case through the application to a non-isothermal continuous stirred tank reactor (CSTR). Finally, the conclusions are given in Section 5.

2. PLSR MODELING

The PLSR model developed here is calculated by simultaneously deflating the data matrices, using the classical PLS-NIPALS algorithm (Geladi and Kowalski, 1986). This procedure gives better results for multivariate prediction and for process monitoring that others alternative PLS algorithms (Gang et al., 2010). Besides, the simultaneous deflation on both data matrices allows the detection of predictor variables that can play an interfering effect (Godoy et al., 2011).

Given a predictor matrix $\mathbf{X}=[\mathbf{x}_1 \ldots \mathbf{x}_N]'$ ($N\times m$), consisting of N samples with m variables per sample, and a response matrix $\mathbf{Y}=[\mathbf{y}_1 \ldots \mathbf{y}_N]'$ ($N\times p$), with p variables per sample, PLSR can be used to find a regression model between the measurement vectors $\mathbf{x}=[x_1\ldots x_m]'$ and $\mathbf{y}=[y_1\ldots y_p]'$, even when their correlation matrixes ($\mathbf{R_x}$ and $\mathbf{R_y}$) are both positive semi-definite (i.e. $\mathbf{X}$ and $\mathbf{Y}$ have collinear variables). The method projects $\mathbf{X}$ and $\mathbf{Y}$ onto correlated low-dimension spaces defined by a common (small) number of A latent variables. The implicit objective of the PLS-NIPALS algorithm in each a-run is to find the solution of the following problem:

$$\max_{\mathbf{w}_a,\,\mathbf{q}_a}\left(\mathbf{w}_a'\mathbf{X}_a'\mathbf{Y}_a\mathbf{q}_a\right) \quad s.t. \quad \|\mathbf{w}_a\|=1,\ \|\mathbf{q}_a\|=1 \qquad (1)$$

where $\mathbf{X}_a$ and $\mathbf{Y}_a$ are the deflated a-versions of $\mathbf{X}_1$=$\mathbf{X}$ and $\mathbf{Y}_1$=$\mathbf{Y}$.

This provides an external, an internal, and a regression model. The external model decomposes $\mathbf{X}$ and $\mathbf{Y}$ in score vectors ($\mathbf{t}_a$ and $\mathbf{u}_a$), weight vectors ($\mathbf{p}_a$ and $\mathbf{q}_a$), and residual error matrices ($\widetilde{\mathbf{X}}$ and $\widetilde{\mathbf{Y}}_2$), as follows:

$$\mathbf{X}=\mathbf{TP}'+\widetilde{\mathbf{X}}=\sum_{a=1}^{A}\mathbf{t}_a\mathbf{p}_a'+\widetilde{\mathbf{X}}=\widehat{\mathbf{X}}+\widetilde{\mathbf{X}}, \qquad (2)$$

$$\mathbf{Y}=\mathbf{UQ}'+\widetilde{\mathbf{Y}}_2=\sum_{a=1}^{A}\mathbf{u}_a\mathbf{q}_a'+\widetilde{\mathbf{Y}}_2=\widehat{\mathbf{Y}}^*+\widetilde{\mathbf{Y}}_2, \qquad (3)$$

where $\mathbf{P}=[\mathbf{p}_1\ldots\mathbf{p}_A]$, $\mathbf{Q}=[\mathbf{q}_1\ldots\mathbf{q}_A]$, $\mathbf{T}=[\mathbf{t}_1\ldots\mathbf{t}_A]$, and $\mathbf{U}=[\mathbf{u}_1\ldots\mathbf{u}_A]$ are orthogonal by columns. Call $\mathbf{R}$ to the pseudo-inverse of $\mathbf{P}'$ ($\mathbf{P}'\mathbf{R}=\mathbf{R}'\mathbf{P}=\mathbf{I}$); then, the prediction of $\mathbf{T}$ is directly obtained from Eq. (2), as: $\mathbf{T}=\mathbf{XR}$, because the row space of $\widetilde{\mathbf{X}}$ belongs to the null-space of the linear transformation $\mathbf{R}'$, i.e. $\widetilde{\mathbf{X}}\mathbf{R}=0$ (Meyer, 2000). If $\mathbf{P}'=\mathbf{W}_A\mathbf{\Sigma}_A\mathbf{V}_A'$ is the compact singular value decomposition (SVD) of $\mathbf{P}'$, then $\mathbf{R}=(\mathbf{P}')^-=\mathbf{V}_A\mathbf{\Sigma}_A^{-1}\mathbf{W}_A'$ where $^-$ denote a generalized inverse (Meyer 2000). Equivalently, from Eq. (3), $\mathbf{S}$ is the pseudo-inverse of $\mathbf{Q}'$ ($\mathbf{Q}'\mathbf{S}=\mathbf{S}'\mathbf{Q}=\mathbf{I}$), and since $\widetilde{\mathbf{Y}}_2\mathbf{S}=0$, then: $\mathbf{U}=\mathbf{YS}$. For the internal model, $\mathbf{t}_a$ is linearly regressed against the y-score vector $\mathbf{u}_a$, i.e.:

$$\mathbf{U}=\mathbf{TB}+\mathbf{H}=\hat{\mathbf{U}}+\mathbf{H}, \quad \mathbf{B}=diag(b_1\ldots b_A) \qquad (4)$$

where $b_1\ldots b_A$ are the regression coefficients determined by minimization of the residual matrix $\mathbf{H}$. Then, the following $\mathbf{X}$-$\mathbf{Y}$ regression model is obtained:

$$\mathbf{Y}=\mathbf{XRBQ}'+\mathbf{HQ}'+\widetilde{\mathbf{Y}}_2=\widehat{\mathbf{Y}}+\widetilde{\mathbf{Y}}_1+\widetilde{\mathbf{Y}}_2 \qquad (5)$$

where $\widetilde{\mathbf{Y}}_2=\mathbf{Y}-\mathbf{YSQ}'$ and $\widetilde{\mathbf{Y}}_1=\mathbf{YSQ}'-\widehat{\mathbf{Y}}$. Also, $\widehat{\mathbf{X}}=\mathbf{XRP'}$ verifies:

$$\widehat{\mathbf{X}}\mathbf{RBQ}'=\mathbf{XRBQ}'=\widehat{\mathbf{Y}} \qquad (6)$$

The selection of A is determined by supervising the simultaneous deflation of $\mathbf{X}$ and $\mathbf{Y}$.

2.1. PLS decomposition of the input and output spaces

After synthesizing an *in-control* PLSR model, the measurement vectors $\mathbf{x}\in\mathbb{R}^m$ and $\mathbf{y}\in\mathbb{R}^p$ can be decomposed as described in the following Lemma (see Proof 1 in Appendix).

Lemma 1. *Call* $\mathbf{\Pi}_{\mathbf{P}|\mathbf{R}^\perp}$ ($\mathbf{\Pi}_{\mathbf{Q}|\mathbf{S}^\perp}$) *the projector on the model subspace* $Span\{\mathbf{P}\}\subseteq\mathbb{R}^m$ ($Span\{\mathbf{Q}\}\subseteq\mathbb{R}^p$)*, along the residual subspace* $Span\{\mathbf{R}\}^\perp$ ($Span\{\mathbf{S}\}^\perp$)*. Then:*

$$\mathbf{\Pi}_{\mathbf{P}|\mathbf{R}^\perp}=\mathbf{PR}', \quad \mathbf{\Pi}_{\mathbf{R}^\perp|\mathbf{P}}=\mathbf{I}-\mathbf{PR}', \qquad (7)$$

$$\mathbf{\Pi}_{\mathbf{Q}|\mathbf{S}^\perp}=\mathbf{QS}', \quad \mathbf{\Pi}_{\mathbf{S}^\perp|\mathbf{Q}}=\mathbf{I}-\mathbf{QS}', \qquad (8)$$

where $^\perp$ *denotes the orthogonal complement of the subspace.*

From Lemma 1, we propose the following theorem on the PLS decomposition (see Proof 2 in Appendix).

Theorem 1. *Input and output variable spaces can be decomposed (by PLSR) in complementary oblique subspaces, with both modeled subspaces interrelated according to:*

$$\begin{gathered}\mathbf{x}=\hat{\mathbf{x}}+\tilde{\mathbf{x}} \in \mathbb{R}^m,\\ \hat{\mathbf{x}}=\mathbf{PR}'\mathbf{x} \in S_{MX}\equiv Span\{\mathbf{P}\},\\ \tilde{\mathbf{x}}=\mathbf{x}-\hat{\mathbf{x}}=(\mathbf{I}-\mathbf{PR}')\mathbf{x} \in S_{RX}\equiv Span\{\mathbf{R}\}^\perp \qquad (9)\end{gathered}$$

$$\begin{gathered}\mathbf{y}=\hat{\mathbf{y}}^*+\tilde{\mathbf{y}}_2 \in \mathbb{R}^p,\\ \hat{\mathbf{y}}^*=\mathbf{QS}'\mathbf{y} \in S_{MY}\equiv Span\{\mathbf{Q}\},\\ \tilde{\mathbf{y}}_2=\mathbf{y}-\hat{\mathbf{y}}^*=(\mathbf{I}-\mathbf{QS}')\mathbf{y}\in S_{RY}\equiv Span\{\mathbf{S}\}^\perp \qquad (10)\end{gathered}$$

$$\begin{gathered}\hat{\mathbf{y}}^*=\hat{\mathbf{y}}+\tilde{\mathbf{y}}_1,\\ \hat{\mathbf{y}}=\mathbf{QBR}'\hat{\mathbf{x}} \in S_{MY},\\ \tilde{\mathbf{y}}_1=\hat{\mathbf{y}}^*-\hat{\mathbf{y}}=\mathbf{QS}'\mathbf{y}-\mathbf{QBR}'\mathbf{x} \in S_{MY} \qquad (11)\end{gathered}$$

The **x** and **y** modeled projections are related to the latent spaces and to each other, as follows:

$$\mathbf{t}=\mathbf{R}'\mathbf{x}=\mathbf{P}'\hat{\mathbf{x}},\quad \hat{\mathbf{u}}=\mathbf{B}\mathbf{t}=\mathbf{S}'\hat{\mathbf{y}},\quad \hat{\mathbf{x}}=\mathbf{P}\mathbf{t},\quad \hat{\mathbf{y}}=\mathbf{Q}\hat{\mathbf{u}},\qquad (12)$$

where $\mathbf{t}=[t_1\cdots t_A]'$ and $\hat{\mathbf{u}}=[\hat{u}_1\cdots\hat{u}_A]'$ are the latent coordinate vectors on the model hyper planes. Hence, their correlation matrixes are related through:

$$\mathbf{\Lambda}=(N-1)^{-1}\mathbf{T}'\mathbf{T}=diag(\lambda_1...\lambda_A)\,,\qquad (13a)$$

$$\mathbf{\Delta}=(N-1)^{-1}\hat{\mathbf{U}}'\hat{\mathbf{U}}=\mathbf{B}\mathbf{\Lambda}\mathbf{B}=diag(\delta_1...\delta_A)\,,\qquad (13b)$$

$$\mathbf{R}_{\hat{\mathbf{x}}}=(N-1)^{-1}\hat{\mathbf{X}}'\hat{\mathbf{X}}=\mathbf{P}\mathbf{\Lambda}\mathbf{P}'\qquad (14a)$$

$$\mathbf{R}_{\hat{\mathbf{y}}}=(N-1)^{-1}\hat{\mathbf{Y}}'\hat{\mathbf{Y}}=\mathbf{Q}\mathbf{\Delta}\mathbf{Q}'\qquad (14b)$$

where λ_i and δ_i are the estimated variances of t_i and $\hat{u}_i$, respectively.

Figure 1 illustrates all the geometric properties mentioned in this work. Each measurement vector is decomposed and their projections are compared with their limits.

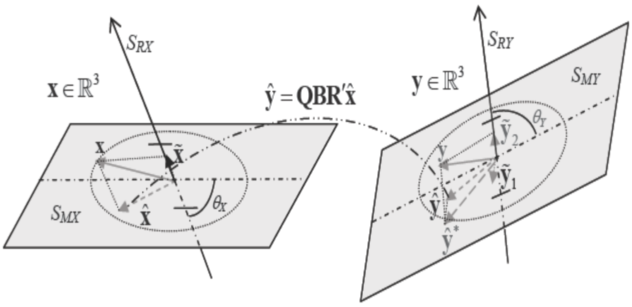

Figure 1: Induced PLS-decomposition with their relations and control limits.

3. PROCESS MONITORING BASED ON PLSR

3.1. Fault detection indexes

The multivariate process monitoring strategy uses statistical indexes associated to each subspace for fault detection. Based on the *in-control* PLSR model, we can analyze any future process behavior by projecting the new **x** and **y** measurements onto each subspace. Thus, for detecting a significant change in S_{MX}, the following Hotelling's T^2 statistic for **t** is defined:

$$T_t^2=\left\|\mathbf{\Lambda}^{-1/2}\mathbf{t}\right\|^2=\left\|\left(\mathbf{\Lambda}^{-1/2}\mathbf{R}'\right)\mathbf{x}\right\|^2=\left\|\left(\mathbf{\Lambda}^{-1/2}\mathbf{P}'\right)\hat{\mathbf{x}}\right\|^2\qquad (15)$$

When a new special event (originally not considered by the in-control PLS model) occurs, the new observation **x** will move out from S_{MX} into S_{RX}. The squared prediction error of **x** (SPE_X), or distance to the **x**-model, is defined as:

$$SPE_X=\left\|\tilde{\mathbf{x}}\right\|^2=\left\|\left(\mathbf{I}-\mathbf{P}\mathbf{R}'\right)\mathbf{x}\right\|^2\qquad (16)$$

Then, SPE_X can be used for detecting a change in S_{RX}. Similarly, the T^2 statistic for $\hat{\mathbf{u}}$, is given by:

$$T_u^2=\left\|\mathbf{\Delta}^{-1/2}\hat{\mathbf{u}}\right\|^2=\left\|\left(\mathbf{\Delta}^{-1/2}\mathbf{S}'\right)\hat{\mathbf{y}}\right\|^2.\qquad (17)$$

In the same way, this statistic can be used for detecting changes in S_{MY}, and the distance to the regression model in S_{MY} is defined by:

$$SPE_{Y1}=\left\|\tilde{\mathbf{y}}_1\right\|^2=\left\|\begin{bmatrix}\mathbf{Q}\mathbf{S}' & -\mathbf{Q}\mathbf{B}\mathbf{R}'\end{bmatrix}\begin{bmatrix}\mathbf{y}\\ \mathbf{x}\end{bmatrix}\right\|^2=\left\|\mathbf{u}-\hat{\mathbf{u}}\right\|^2\qquad (18)$$

and the distance to the **y-**model in S_{RY} is defined as:

$$SPE_{Y2}=\left\|\tilde{\mathbf{y}}_2\right\|^2=\left\|\left(\mathbf{I}-\mathbf{Q}\mathbf{S}'\right)\mathbf{y}\right\|^2.\qquad (19)$$

Frequently, $\mathbf{R}_{\hat{\mathbf{x}}}$ and $\mathbf{R}_{\hat{\mathbf{y}}}$ are singular. Then, the generalized Mahalanobis' distance for $\hat{\mathbf{x}}$ and $\hat{\mathbf{y}}$ are:

$$D_{\hat{\mathbf{x}}}=\hat{\mathbf{x}}'\mathbf{R}_{\hat{\mathbf{x}}}^{-}\hat{\mathbf{x}}\,,\qquad (20a)$$

$$D_{\hat{\mathbf{y}}}=\hat{\mathbf{y}}'\mathbf{R}_{\hat{\mathbf{y}}}^{-}\hat{\mathbf{y}}\,.\qquad (20b)$$

Besides, Proof 3 in Appendix demonstrate the following

Theorem 2. *The metrics on* $\hat{\mathbf{x}}$, $\mathbf{t}$, $\hat{\mathbf{u}}$ *or* $\hat{\mathbf{y}}$ *are equivalents, i.e.:* $D_{\hat{\mathbf{x}}}=T_t^2=T_u^2=D_{\hat{\mathbf{y}}}$.

The above theorem 2 tells that output variables can be monitored through a PLSR-based metric of the input variables. Therefore, we propose monitoring using four non-overlapped metrics (SPE_X, T_t^2, SPE_{Y1}, and SPE_{Y2}) which completely cover both measurement spaces, each one on a different subspace.

3.2. Fault diagnosis by means of alarmed subspaces

An anomaly is a change in the measurements following or not the correlation structure captured by the PLSR model. If the change produces an out-of-control point, the anomaly source can be classified according to a) an excessively large operation change of the normal operation; b) a significant increase of variability; c) the alteration of cross-correlations, and d) sensor faults. Cases a) and b) involve changes in the measurement vector following the modeled correlation structure; while cases c) and d) involve changes in some variables altering the correlation pattern with the others. In fact, an abnormal process behavior involves a deviation of the modeled correlations, thus increasing the value of the proper metric being used. In order to classify the abnormalities, we analyze the effect on each subspace (see Table 1). Rows 1), 2), 3) and 6) feature complex process changes; while rows 4) and 5) represent localized sensor faults. By analyzing the contributions to an alarmed index (Alcala and Qin, 2011), such as SPE_X (or SPE_Y), it could be possible to discriminate changes in the **X**- / **Y**-outer part against sensor fault in **x** / **y** (see this ambiguity in Table 1).

In summary, the proposed monitoring strategy is based on an input and output space PLS decomposition, which classifies the type of process fault or anomaly according to the statistic that triggers the alarm condition.

Table 1. Fault diagnosis based on alarmed index.

Fault/Anomaly in	T_t^2	SPE_X	SPE_{Y1}	SPE_{Y2}
1- Inner part, d**B**	–	–	×	–
2- **X** outer part, d**P**	–	×	o	–
3- **Y** outer part, d**Q**	–	–	o	×
4- **x** sensor	–	×	o	–
5- **y** sensor	–	–	o	×
6- latent space upset	×	–	–	–

×: high value. –: negligible value. o: high/low value.

4. SIMULATION EXAMPLES

4.1. A numerical evaluation example

To understand the proposed decompositions and statistics as monitoring tools, we simulated different faults in a synthetic system. The system includes an internal and an external part and an input-output relation given by:

$$\mathbf{t} = \mathbf{t}^0 + \boldsymbol{\xi}, \quad \boldsymbol{\xi} \sim N\left(\mathbf{0}, 0.1^2\,\mathbf{I}_2\right),$$

$$\mathbf{u} = \mathbf{B}\mathbf{t} + \boldsymbol{\gamma}, \quad \mathbf{B} = diag\left(2,\, 0.5\right),\ \boldsymbol{\gamma} \sim N\left(\mathbf{0}, 0.05^2\,\mathbf{I}_2\right),$$

$$\mathbf{x} = \mathbf{P}\mathbf{t} + \tilde{\mathbf{x}}, \quad \mathbf{P} = \left[\mathbf{p}_1 \quad \mathbf{p}_2\right],\ \tilde{\mathbf{x}} \sim N\left(\mathbf{0}, 0.05^2\,\mathbf{I}_7\right),$$

$$\mathbf{y} = \mathbf{Q}\mathbf{u} + \tilde{\mathbf{y}}_2,\ \mathbf{Q} = \left[\mathbf{q}_1 \quad \mathbf{q}_2\right],\ \tilde{\mathbf{y}}_2 \sim N\left(\mathbf{0}, 0.05^2\,\mathbf{I}_3\right),$$

$$\hat{\mathbf{y}}^* = \mathbf{Q}\mathbf{B}\mathbf{R}'\mathbf{x} + \mathbf{Q}\boldsymbol{\gamma},\ \mathbf{p}_i = \mathbf{p}_i^* \big/ \left\|\mathbf{p}_i^*\right\|,\ \mathbf{q}_j = \mathbf{q}_j^* \big/ \left\|\mathbf{q}_j^*\right\|,$$

$$\mathbf{p}_1^* = \left[1.5, 0, 2, 1, 0.5, 0, 2.5\right]',$$

$$\mathbf{p}_2^* = \left[0, 2.5, 0.5, -0.5, -1.0, 1.5, 0\right]',$$

$$\mathbf{q}_1^* = \left[1.5, 1, 0.5\right]', \qquad \mathbf{q}_2^* = \left[0, 0.5, -1\right]',$$

where $\mathbf{R}'$ is the pseudo-inverse of **P**. The normal process operation follows a sequence of 4 states: $\left\{\left(t_1^0, t_2^0\right)\right\}_{1\ldots4} = \left\{(1,1),(1,3),(3,3),(3,1)\right\}$. Matrixes **X** and **Y** are obtained on the basis of 32 realizations of **x** and **y**. The PLSR model was adjusted with centered data, without scaling, to identify a centered version of the latent process. The differences between the identified matrixes and the true ones are negligible, although the columns of $\hat{\mathbf{R}}$ and $\hat{\mathbf{Q}}$ may include opposite signs to those of **R** and **Q**. Since such sign alteration is present in both matrixes, then: $\mathbf{Q}\mathbf{B}\mathbf{R}' \cong \hat{\mathbf{Q}}\hat{\mathbf{B}}\hat{\mathbf{R}}'$. Since $\hat{\mathbf{y}} = \sum_{a=1}^{A} b_a \mathbf{q}_a \mathbf{r}_a' \mathbf{x}$, when $\hat{u}_2$ exhibits an opposite sign to that of the real u_2 (e.g., because $\hat{\mathbf{r}}_2 = -\mathbf{r}_2$), then $\hat{\mathbf{q}}_2 = -\mathbf{q}_2$. Six faults were simulated (see Table 1): 1) a change of the internal model at k=11: $db_2 = 0.7\ b_2$; 2) a change of the process coefficient (plant) at k=19, given by $d\mathbf{p}_2$ = [0, 0.32, 0, 0,-0.08, 0.16, -0.16]' (high SPE_X if $d\mathbf{p}_2 \in S_{RX}$), and at k=27; 3) $d\mathbf{q}_1$ = [-0.08, 0.06, 0]' (high SPE_{Y2} if $d\mathbf{q}_1 \in S_{RY}$); 4) a multiple sensor fault in the measurement **x** at k = 35, given by **x = x +** d**x**, with $d\mathbf{x} = [0.25\ \ 0\ \ 0\ \ 0\ \ 0\ \ 0.25\ \ 0]'$; 5) a multiple sensor fault in the measurement **y** at k=43, with $d\mathbf{y} = [-0.23, 0.27, 0.14]' \in S_{RY}$, and 6) a change (following the modeled correlation structure) at k = 51, given by $d\hat{\mathbf{x}}$ = [0, 3.1623, 0.6325, -0.6325, -1.2649, 1.8974, 0]'≡ **P** [0 4]'. Table 1 shows the diagnosis expected in each simulated fault/anomaly. Figure 2 shows the evolution of each statistic with time, where it is possible to detect and classify the type of simulated fault on the basis of the information given in Table 1.

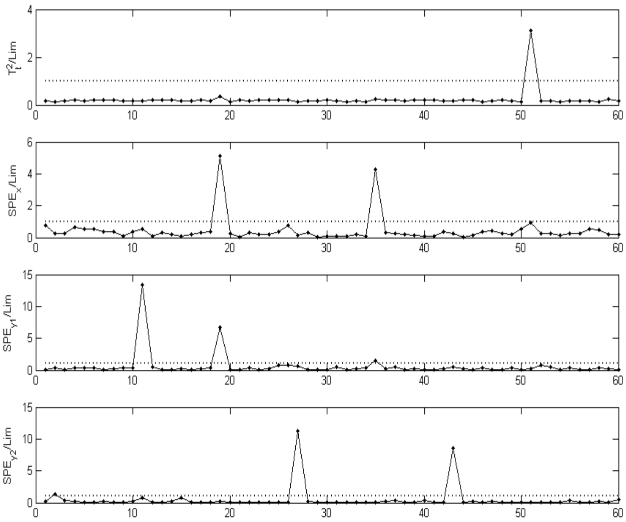

Figure 2: Time evolution of each normalized PLSR-statistic.

4.2. Monitoring of a controlled reactor

A simulated case study is used to evaluate the performance of the proposed monitoring technique for a variety of fault scenarios. The process is a continuous stirred tank reactor (CSTR) with a cooling jacket. The chemical kinetics is characterized by a classical first-order irreversible reaction A→B. The instrumentation includes level, flow rate and temperature transmitters and two PI controllers, with set-points SP_T and SP_h. The controlled variables are the reactor temperature (T) and the tank level (h). The manipulated variables are the coolant flow-rate (Q_J) and the output flow-rate from the reactor (Q). Input conditions T_F, T_{JF}, and C_{AF} are assumed constant to the values in Table 2. Figure 3 shows a schematic diagram of the reactor.

The mathematical model of the system is represented by (Singhal and Seborg, 2002):

$$\frac{dC_A}{dt} = -k_0 e^{-E/RT} C_A + \frac{Q_F C_{AF} - Q C_A}{Ah},$$

$$\frac{dT}{dt} = \frac{(-\Delta H) k_0 e^{-E/RT} C_A}{\rho C_p} + \frac{Q_F T_F - QT}{Ah} + \frac{UA_J\left(T_J - T\right)}{\rho C_p A h},$$

$$\frac{dT_J}{dt} = \frac{Q_J\left(T_{JF} - T_J\right)}{V_C} + \frac{UA_J\left(T - T_J\right)}{\rho_J C_{pJ} V_C},$$

$$\frac{dh}{dt} = \frac{Q_F - Q}{A},$$

$$\frac{dQ_J}{dt} = K_{C1}\frac{d(SP_T - T)}{dt} + \frac{K_{C1}}{T_{i1}}(SP_T - T),$$

$$\frac{dQ}{dt} = K_{C2}\frac{d(SP_h - h)}{dt} + \frac{K_{C2}}{T_{i2}}(SP_h - h),$$

$$x = \frac{C_{AF} - C_A}{C_{AF}}, \qquad \dot{H} = \Delta H\, k_0 e^{-E/RT} C_A A h\,.$$

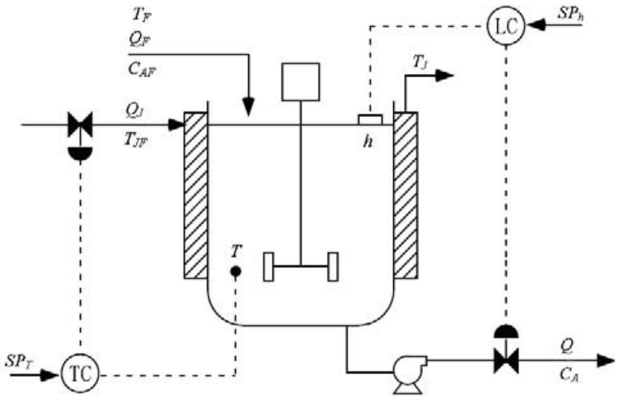

Figure 3: Schematic of the CSTR system with a multi-loop control system.

Table 2: Nominal Operating Conditions and Model Parameters for the CSTR in Fig. 3

Q = 100 L/min	$A = 0.1666$ m^2
Q_J = 15 L/min	$k_0 = 7.2 \times 10^{10}$ min^{-1}
T_F = 320 °K	$\Delta H = -5 \times 10^4$ J/mol
T_{JF} = 300 °K	ρC_p = 239 J/(L °K)
T = 402.35 °K	$\rho_J C_{pJ}$ = 4175 J/(L °K)
T_J = 345.44 °K	E/R = 8750 °K
C_{AF} = 1.0 mol/L	$UA_J = 5 \times 10^4$ J/(min °K)
C_A = 0.037 mol/L	V_J = 10 L
h = 0.6 m	$K_{C1} = -1$, $T_{i1} = 1$, $K_{C2} = -15$, T_{i2}=10,

Since data are auto-correlated, **X** and **Y** include time-lagged measurements to a given order. Notice that PLSR modeling works in this case as an alternative identification method for discrete dynamics like ARX. In this application, the adopted ARX order is 3, so the representation takes the form

$$\hat{\mathbf{y}}(k) = [\mathbf{QBR'}]\mathbf{x}(k) = [\mathbf{B}_1\mathbf{A}_1\mathbf{A}_2\mathbf{A}_3]\begin{bmatrix}\mathbf{z}(k-1)\\ \mathbf{y}(k-1)\\ \mathbf{y}(k-2)\\ \mathbf{y}(k-3)\end{bmatrix} =$$

$$= \mathbf{B}_1\mathbf{z}(k-1) + \mathbf{A}_1\mathbf{y}(k-1) + \mathbf{A}_2\mathbf{y}(k-2) + \mathbf{A}_3\mathbf{y}(k-3) \quad (21)$$

where $\mathbf{y} = \left[Q_J \quad Q \quad C_A \quad T \quad T_J \quad h \quad x \quad \dot{H}\right]'$ and $\mathbf{z} = \left[SP_T \quad SP_h \quad Q_F\right]'$ are centered and scaled. The sampling time is adjusted to T_s=5 min, a quite reasonable time interval considering an approximated settling time of T_{st}=120 min. To build the identification data set, 50 random set-point changes, each one every 120 min., around the nominal values are implemented, and the step responses of the system were collected along 120 min after each step change. The input variables in **z** followed uniform distributions around the nominal value, with ranges SP_h: 0.6 ± 0.05 m, SP_T: 402.35 ± 3 °K, and Q_F: 100 ± 5 L/min. The dynamic in Eq. (21) is adjusted by PLSR modeling and gave a standard error of = 4.2%. The determined model order is A=5 and, the post modeling verification with the Variable Importance in Projection Index (VIP) - for each x_i (i=1…27) - gives greater than 0.8 for all of them, indicating that all the used predictors are significant (Godoy et al., 2011).

Figure 4 shows the time evolution of each statistic normalized by its control limit, which clearly exhibit the four simulated abnormalities (see Table 3). In the samples k = 121, 122 and 123, the discrete ARX model fails to follow the fast change experienced by the continuous process, resulting in a high SPE_{Y1}, SPE_{Y2}, SPE_X. During the first transition (starting at k = 121) K_{C2} is away from the proper tuning. On the contrary, during the second transition (starting at k = 141) K_{C2} is close to the right tuning. Thus, the control system takes a longer time for stabilizing the controlled variables during the first transition than when the process system goes back to the previous condition (see Fig. 4a).

Table 3: Simulated fault scenarios.

Type	**Location**	**Magnitude**	**Diagnosis**
sensor fault	k=21..41	dQ_F=20 L/min	2/4
sensor fault propagated	k=71..91	dh = 0.15 m	6 and 3/5
system fault	k=121..141	dK_{C2} = -0.75	3/5→6
process fault -disturbance	k=171..191	dk_0= 0.36 10^{10} min^{-1}	3/5

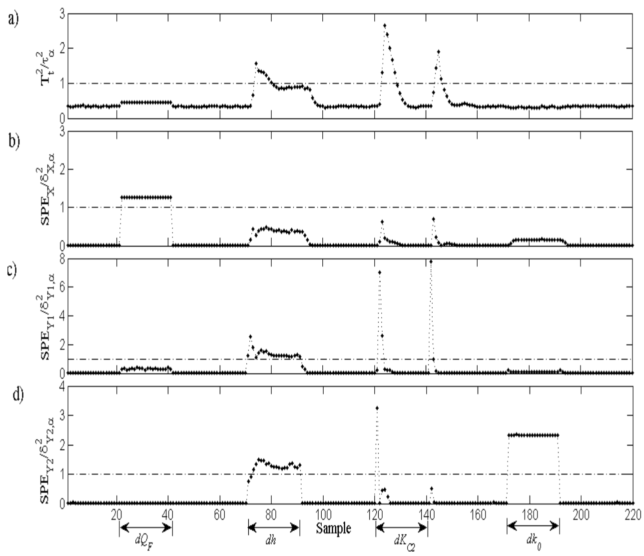

Figure 4: Simulation of statistical monitoring during 4 different faults on the closed-loop operation of CSTR.

The simulation results show that the developed prototypes are able to identify abnormalities attributed to poor control performance, process upsets and disturbances, as well as sensor faults. The general approach proposed for closed-loop monitoring is based on designing a PLSR model that should be then used online to identify abnormalities. The model supporting this monitoring approach is based on operating data taken along periods where the controller is assumed to be working satisfactorily. Process data recollection constitutes a critical step when developing empirical models for monitoring control performances; it is highly desirable to be operating as close as possible to an optimal condition during the period in which the controlled process data is collected.

5. CONCLUSIONS AND FUTURE WORKS

The multivariate process monitoring approach proposed in this work is based on a PLSR model that represents 'in-control' conditions. Thus, a meaningful deviation of the variables from their expected trajectories serves for the detection and diagnosis of abnormal process behaviors. The results obtained using two simulation examples illustrate that the proposed strategy is efficient and accurate enough as to deserve additional future work. In particular, a controlled CSTR is successfully monitored during different fault conditions or process abnormalities using the new detection indices. The combination of alarm/no-alarm conditions occurring during the simultaneous use of the proposed indices can be used for locating and classifying the disturbing event and contributes to a preliminary diagnosis.

ACKNOWLEDGMENTS

The authors are grateful for financial support received from CONICET, MinCyT, Universidad Nacional del Litoral, and Uni. Tecnológica Nacional (Argentina).

APPENDIX A

Proof 1. The oblique projector onto $Span\{\mathbf{A}\}$ along $Span\{\mathbf{B}\}$ can be obtained by the following equation (Meyer, 2000):

$$\mathbf{\Pi}_{\mathbf{A}|\mathbf{B}} = \mathbf{A}\left(\mathbf{A}'\mathbf{\Pi}_{\mathbf{B}}^{\perp}\mathbf{A}\right)^{-1}\mathbf{A}'\mathbf{\Pi}_{\mathbf{B}}^{\perp} \qquad \text{(A1)}$$

where $\mathbf{\Pi}_{\mathbf{B}}^{\perp}$ is the orthogonal projector onto $Span\{\mathbf{B}\}^{\perp}$. Since $\mathbf{R}$ and $\mathbf{S}$ are full-column-ranked, then:

$$\mathbf{\Pi}_{\mathbf{R}^{\perp}}^{\perp} = \mathbf{\Pi}_{\mathbf{R}} = \mathbf{R}\left(\mathbf{R}'\mathbf{R}\right)^{-1}\mathbf{R}' = \mathbf{R}\mathbf{R}', \qquad \text{(A2)}$$

$$\mathbf{\Pi}_{\mathbf{S}^{\perp}}^{\perp} = \mathbf{\Pi}_{\mathbf{S}} = \mathbf{S}\left(\mathbf{S}'\mathbf{S}\right)^{-1}\mathbf{S}' = \mathbf{S}\mathbf{S}'. \qquad \text{(A3)}$$

Since $\mathbf{P}'\mathbf{R} = \mathbf{R}'\mathbf{P} = \mathbf{I}$ (or $\mathbf{Q}'\mathbf{S} = \mathbf{S}'\mathbf{Q} = \mathbf{I}$), then Eq. (A1) and Eq. (A2) [or Eq. (A3)] yield: $\mathbf{\Pi}_{\mathbf{P}|\mathbf{R}^{\perp}} = \mathbf{P}\mathbf{R}'$ (or $\mathbf{\Pi}_{\mathbf{Q}|\mathbf{S}^{\perp}} = \mathbf{Q}\mathbf{S}'$). Similarly, we have $\mathbf{\Pi}_{\mathbf{R}^{\perp}|\mathbf{P}} = \mathbf{I} - \mathbf{P}\mathbf{R}'$ (or $\mathbf{\Pi}_{\mathbf{S}^{\perp}|\mathbf{Q}} = \mathbf{I} - \mathbf{Q}\mathbf{S}'$). □

Partially, Lemma 1 has already been proved by Gang et al., 2010). Each oblique projector in Eq. (7, 8) works as an identity matrix applied onto every vector belonging to its range.

Proof 2. Eqs. (9, 10) can be proved by taking into account that: (i) $Span\{\mathbf{I} - \mathbf{P}\mathbf{R}'\} = Span\{\mathbf{R}\}^{\perp}$ and $Span\{\mathbf{I} - \mathbf{Q}\mathbf{S}'\} = Span\{\mathbf{S}\}^{\perp}$ (see Lemma 1); and (ii) the projections belong to complementary subspaces, because $rank\left(\mathbf{P}\mathbf{R}'\left(\mathbf{I} - \mathbf{P}\mathbf{R}'\right)\right) = \dim(S_{MX}) + \dim(S_{RX})$ $= m$ and $rank\left(\mathbf{Q}\mathbf{S}'\left(\mathbf{I} - \mathbf{Q}\mathbf{S}'\right)\right) = \dim\left(S_{MY}\right) + \dim\left(S_{RY}\right) = p$. Then, Eq. (11) is directly derived from Eq. (6). □

Proof 3. Since $\mathbf{Q}$ is orthogonal by columns, the property of the generalized inverse of a SVD yields: $\mathbf{R}_{\hat{\mathbf{y}}}^{-} = \left(\mathbf{Q}\mathbf{\Delta}\mathbf{Q}'\right)^{-} = \mathbf{Q}\mathbf{\Delta}^{-1}\mathbf{Q}'$. Then, from Eq. (20b): $D_{\hat{\mathbf{y}}} = \hat{\mathbf{y}}'\mathbf{R}_{\hat{\mathbf{y}}}^{-}\hat{\mathbf{y}} = \hat{\mathbf{y}}'\mathbf{Q}\mathbf{\Delta}^{-1}\mathbf{Q}'\hat{\mathbf{y}} = \hat{\mathbf{u}}'\mathbf{\Delta}^{-1}\hat{\mathbf{u}} = T_u^2$. Equivalently, by replacing $\mathbf{R}_{\hat{\mathbf{x}}}^{-} = \left(\mathbf{P}\mathbf{\Lambda}\mathbf{P}'\right)^{-} = \mathbf{P}\mathbf{\Lambda}^{-1}\mathbf{P}'$ into Eq. (20a), the distance results: $D_{\hat{\mathbf{x}}} = \hat{\mathbf{x}}'\mathbf{R}_{\hat{\mathbf{x}}}^{-}\hat{\mathbf{x}} = \hat{\mathbf{x}}'\mathbf{P}\mathbf{\Lambda}^{-1}\mathbf{P}'\hat{\mathbf{x}} = T_t^2$. Furthermore, by combining Eqs. (12, 13, 14, 17), $T_u^2 = \mathbf{t}'\mathbf{B}\mathbf{B}^{-1}\mathbf{\Lambda}^{-1}\mathbf{B}^{-1}\mathbf{B}\mathbf{t} = T_t^2$ is obtained. From all these equalities, Proposition 1 is proven. □

REFERENCES

Alcala C.F. and Qin S.J., 2011. Analysis and generalization of fault diagnosis methods for process monitoring. *J. Process Control* 21, 322-330.

AlGazzawi A. and Lennox B., 2009. Model predictive control monitoring using statistics. *J. Process Control* 19, 314-327.

Gang L.G., Qin S.J. and Zhou D., 2010. Geometric properties of partial least squares for process monitoring. *Automatica* 46, 204-210.

Geladi P. and Kowalski B., 1986. Partial least-squares regression: A tutorial. *Anal. Chim. Acta*, 185, 1-17.

Godoy J.L., Minari R.J., Vega J.R., Marchetti J.L., 2011. Multivariate Statistical Monitoring of an Industrial SBR Process. Soft-sensor for Production and Rubber Quality. *Chem. Intell. Lab. Syst.* DOI: 10.1016/j.chemolab.2011.04.008.

Laurí D., Rossiter J.A., Sanchis J., Martínez M., 2010. Data-driven latent-variable model-based predictive control for continuous processes. *J. Process Control* 20, 1207–1219.

Meyer D., 2000. *Matrix analysis and applied linear algebra*. SIAM, USA.

Singhal A. and Seborg D.E., 2002. Pattern Matching in Multivariate Time Series Databases Using a Moving-Window Approach. *Ind. Eng. Chem. Res.* 41, 3822-3838.